**Immunology Research and Perspectives**

https://irp.cultechpub.com/irp

Cultech Publishing

*Article*

# Immunoinformatics-Driven Design of a Self-Amplifying mRNA Vaccine Against Human Herpesvirus 6 Advancing Viral Immunoprophylaxis

**Wassef Ullah***

Department of Biochemistry, Abdul Wali Khan University, Mardan, Pakistan

*Corresponding author: Waseef Ullah, waseefullah@awkum.edu.pk

**Abstract**

Human Herpesvirus 6 (HHV-6) is a common virus characterized by its double-stranded DNA structure that infects almost everyone by early childhood. While usually mild, HHV-6 poses serious health threats to people with weakened immune systems, contributing to neurological issues like encephalitis and adding complications in organ transplant cases. Despite its ubiquity and potential risks, there is currently no licensed vaccine to prevent either HHV-6 infection or reactivation. In this study, an immunoinformatics and reverse vaccinology approach was employed to design a self-amplifying mRNA (saRNA) multi-epitope vaccine targeting HHV-6. Four immunogenic viral proteins were screened, leading to the identification of 8 B-cell epitopes, 8 cytotoxic T lymphocyte (CTL) epitopes, and 8 helper T lymphocyte (HTL) epitopes, all exhibiting strong antigenicity and non-allergenic, non-toxic profiles. These epitopes were assembled into four vaccine constructs using optimized linkers and adjuvanted with the 50S ribosomal L7/L12 protein to enhance immunogenicity. Among the constructs, V3 demonstrated the most favorable physicochemical properties and structural stability. Molecular docking analyses revealed strong binding of V3 with Toll-like receptor 4 (TLR4), achieving a ClusPro docking score of -361.46 and a HADDOCK score of -5.3 ± 4.1, supported by stable electrostatic and van der Waals interactions. Normal mode analysis (NMA) confirmed the structural stability of the V3-TLR4 complex, with a low eigenvalue indicative of favorable conformational dynamics. Immune simulations using C-ImmSim predicted robust primary, secondary, and tertiary immune responses, characterized by immunoglobulin class switching, memory B- and T-cell generation, and a Th1-biased cytokine profile. Codon optimization and *in silico* cloning further validated the feasibility of vaccine expression and downstream experimental testing. Collectively, these findings highlight the potential of the proposed HHV-6 saRNA multi-epitope vaccine as a promising prophylactic candidate, warranting further *in vitro* and *in vivo* validation.

**Keywords**

Human herpesvirus 6, Self-amplifying mRNA vaccine, Multi epitope vaccine, Immunoinformatics, Reverse vaccinology

**Article History**

Received: 01 December 2025 Revised: 02 March 2026

Accepted: 25 May 2026 Available Online: 28 May 2026

## 1. Introduction

Human Herpesvirus 6 (HHV-6) is a widely distributed DNA virus classified within the Herpesviridae family and exists in two closely related variants, HHV-6A and HHV-6B. This virus is highly prevalent worldwide, with nearly all individuals acquiring it early in life [1]. Following initial infection, HHV-6 establishes latency, primarily in monocytes, macrophages, and T cells, allowing it to persist in the host for life. Although often asymptomatic, HHV-6 can reactivate under immune-compromised conditions, leading to serious complications, particularly in organ transplant recipients and patients with weakened immune systems. The virus has been linked to conditions such as encephalitis, hepatitis, and myocarditis, and is suspected to contribute to certain chronic diseases and neurological conditions. Given its ability to remain latent and reactivate, as well as its integration into human chromosomes, HHV-6 poses a unique challenge in public health, especially in vulnerable populations [2].

HHV-6 Primary infection typically occurs during early childhood, most commonly before the age of two years, and is often associated with mild or self-limiting clinical manifestations such as febrile illness or exanthema subitum (roseola infantum). Seroprevalence studies indicate that HHV-6 exposure is nearly universal across diverse geographic regions, including North America, Europe, Asia, Africa, and South America. Following primary infection, HHV-6 establishes lifelong latency in various host cells, including monocytes, macrophages, and T lymphocytes. Reactivation of latent HHV-6 is frequently observed in immunocompromised individuals, particularly hematopoietic stem cell and solid-organ transplant recipients, patients undergoing chemotherapy, and individuals with advanced immunodeficiency. In these populations, HHV-6 reactivation has been associated with severe clinical outcomes, including encephalitis, bone marrow suppression, graft rejection, hepatitis, myocarditis, and increased mortality. A unique epidemiological feature of HHV-6 is its ability to integrate into human chromosomes, a phenomenon known as chromosomally integrated HHV-6, which occurs in approximately 0.5-1% of the global population and can be vertically transmitted. This integration complicates diagnosis and may influence disease severity and reactivation risk. Given its high prevalence, lifelong persistence, potential for reactivation, and lack of a licensed vaccine, HHV-6 represents a significant and underrecognized public health concern, particularly among vulnerable populations.With the limitations of existing antiviral therapies and the lack of a licensed vaccine for HHV-6, the development of an effective prophylactic measure is crucial. In this study, a computational immunoinformatics methodology was used to design a multiepitope self-amplifying mRNA (saRNA) vaccine targeting HHV-6. The creation of saRNA vaccines provides numerous benefits, such as rapid production and the ability to encode multiple epitopes within a single construct. By leveraging immunoinformatics, we identified and screened epitopes with the highest prospective to bring strong and specific immune responses, ultimately creating a vaccine construct that could offer comprehensive and targeted protection against HHV-6.

Messenger RNA (mRNA) vaccines have materialized as a groundbreaking platform for preventing infectious diseases, leveraging their ability to deliver mRNA into host cells, where it is translated into pathogen-specific antigenic proteins to stimulate targeted immune responses [3,4]. These vaccines remain lauded for their safety, versatility, rapid development, and capacity to provoke mutually humoral and cellular immunity. The remarkable success of mRNA vaccines in addressing SARS-CoV-2 has sparked interest in their application to other pathogens [5], including HHV-6. HHV-6 produces several proteins that contribute to its infection and immune evasion strategies, making it a prime target for vaccine development. However, single-protein immunization strategies often fall short of providing comprehensive protection, necessitating a multivalent methodology.

Current study uses advanced an innovative multivalent saRNA vaccine targeting HHV-6, designed to express key viral antigens involved in infection and immune system evasion. The vaccine construct incorporates epitopes linked by a flexible Glutamic acid-Alanine-Alanine-Alanine-Lysine (EAAAK), Alanine-Alanine-Tyrosine (AAY), Glycine-Proline-Glycine-Proline-Glycine (GPGPG), and Lysine-Lysine (KK) linkers, ensuring optimal antigen folding and functional expression in a single sequence. Advanced immunoinformatics tools guided the selection of these epitopes to ensure high immunogenicity, safety, and antigen specificity.

Preclinical evaluation of the vaccine demonstrated its capability to stimulate robust antibody retorts and antigen-specific T-cell immunity [6]. *In silico* analyses, including molecular docking normal mode analysis (NMA) and immune simulations, confirmed durable binding to immune receptors and predicted a potent and stable immune response. These outcomes recommend that the vaccine devours the prospective to provide comprehensive protection against HHV-6 infection and reactivation. This work signifies a substantial step onward in the design of saRNA vaccines and highlights a promising candidate for combating HHV-6, a pathogen with substantial public health implications.

## 2. Materials and Methods

### 2.1 Sequence Retrieval

To identify and retrieve the amino acid sequences for target proteins, The UniProt database ( https://www.uniprot.org ) was utilized [7]. Specifically, sequences of key proteins from HHV-6A (Proteome ID: UP000008227) were selected, including Envelope Glycoprotein B (UniProt ID: Q9QNC8), Envelope Glycoprotein H (UniProt ID: Q9QNC5), Envelope Glycoprotein L (UniProt ID: Q9QNC9), and the Major Capsid Protein (UniProt ID: Q9QND4). Each sequence was downloaded in FASTA format to facilitate detailed analysis.Antigenic possessions of these proteins remained subsequently projected using the VaxiJen tool (http://www.ddg-pharmfac.net/vaxijen/VaxiJen/VaxiJen.html) [8], which is based on a physicochemical algorithm for determining antigenic potential. Additionally, AllerTop v2.0 (https://www.ddg-pharmfac.net/AllerTOP/) [9], a tool leveraging a fingerprint-based descriptor technique, was used to evaluate allergenic potential. To minimize the risk of autoimmune reactions and host cross-reactivity, host non-homology analysis was conducted using BLASTp (https://blast.ncbi.nlm.nih.gov/Blast.cgi) against the Homo sapiens reference proteome. Searches were performed using default parameters with an E-value cutoff of 1e-3, and proteins showing >30% sequence identity and >70% query coverage were excluded. BLASTp was selected due to its widespread use and reliability in identifying sequence-level homology relevant to immune cross-reactivity in immunoinformatics-based vaccine design [10] (Figure 1).

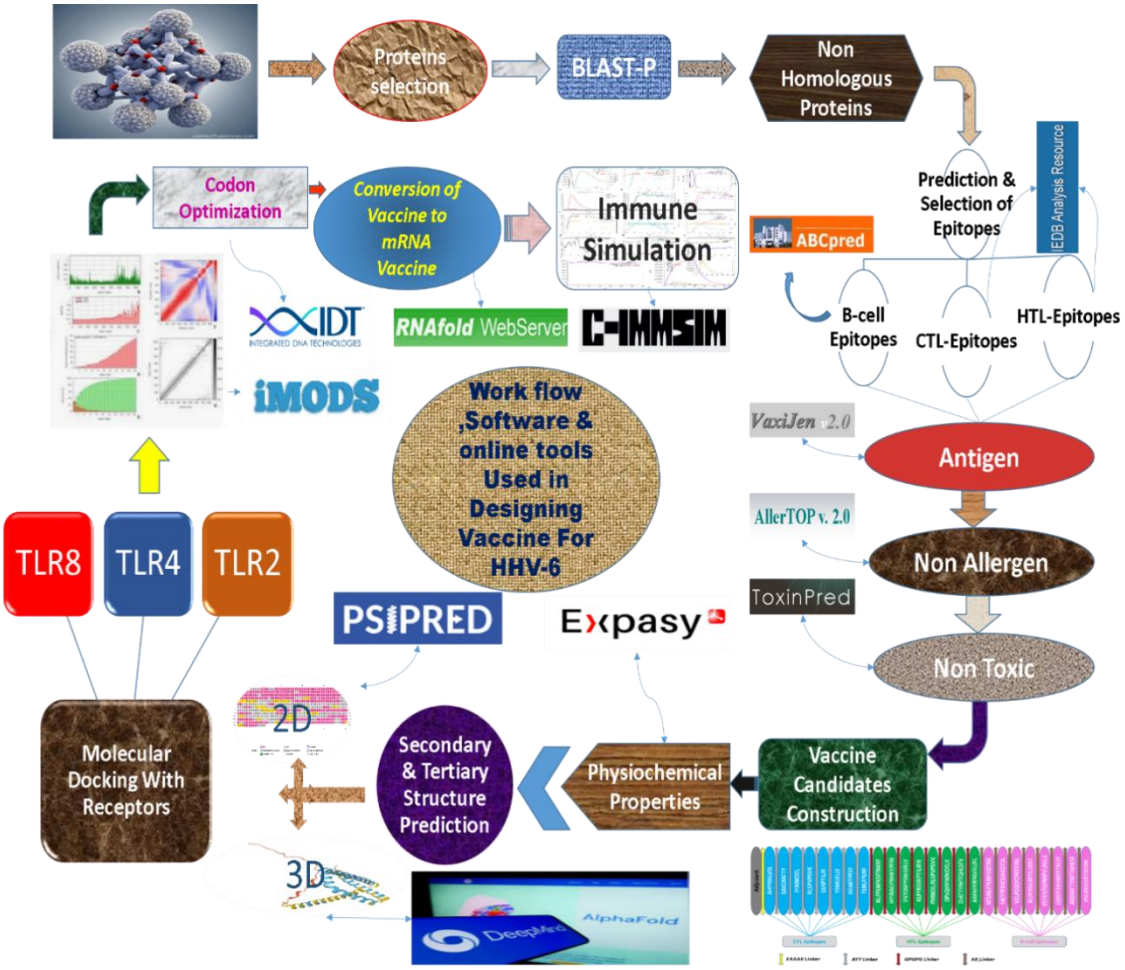


**Figure 1.** A graphic overview of our multi-epitope self-amplifying vaccine design process, information on databases, software, and web services used in our research.

### 2.2 Prediction of B-Cell Epitopes

To explore the immune-stimulating potential of the selected proteins, current study focused on predicting B-cell epitopes, which are instrumental in activating humoral immunity and enhancing pathogen defense through antibody response [11]. Using the ABCpred server [12,13], which applies a neural network approach, identified 16-mer B-cell epitopes with a

cut-off score of 0.51. This method offers refined predictions by considering key factors, such as specificity, compassion, accuracy, and confidential predictive value, to ensure high reliability in epitope identification [14].

### 2.3 Cytotoxic T-Lymphocyte Cell Epitope Prediction

The initial step in sparking the host immune feedback against diseases involves presenting antigens to cytotoxic T lymphocyte (CTL) through major histocompatibility Class-I (MHC-I). Leveraging the IEDB (https://tools.iedb.org/mhci/) consensus algorithm and all available human leukocyte antigen (HLA) leukocyte antigens, which pinpointed MHC class-I binding epitopes [15]. This entailed utilizing diverse human MHC-I binding alleles to identify epitopes with significant immunogenicity for stimulating $CD8^+$ T lymphocytes. Prioritizing epitopes with an IC50 < 100 nm, our focus was on these highly promising candidates for inclusion in vaccine design.

### 2.4 Helper T Lymphocyte Epitope Prediction

To initiate both cellular and humoral immune responses, The NetMHCIIpan2.1 server (https://services.healthtech.dtu.dk/service.php?NetMHCIIpan-2.1) was utilized to predicted helper T lymphocyte (HTL) epitopes [16]. This server analyzes MHC-II peptide binding to identify epitopes with strong binding affinity to specific alleles. Candidate peptides were ranked based on binding strength, least percentile rank, and great prediction scores, allowing us to prioritize epitopes with the highest potential to effectively trigger immune responses.

### 2.5 Evaluation of Predicted Epitopes

To guarantee the safety and efficacy of the selected B- and T-cell epitopes, a series of evaluations was performed. Allergenicity was first assessed using AllerTop v2.0 (https://www.ddg-pharmfac.net/AllerTOP/) [9], which predicts potential allergens using a fingerprint-based algorithm. VaxiJen v2.0 (http://www.ddg-pharmfac.net/vaxijen/VaxiJen/VaxiJen.html) to evaluate antigenicity, selecting epitopes with a minimum probability threshold of 0.4 to prioritize highly antigenic candidates [8]. Lastly, the ToxinPred2 (https://webs.iiitd.edu.in/raghava/toxinpred2/) [17] server was utilized to screen for potential toxicity, helping us identify safe components with the highest potential for vaccine development.

### 2.6 Construction of Final Vaccine

All epitopes selected from the preceding immunoinformatics analyses were assembled into a single cohesive multi-epitope subunit vaccine construct. The design incorporated CTL, HTL, and B-cell (BCL) epitopes, along with an immunostimulatory adjuvant, to ensure balanced activation of cellular and humoral immune responses. To maintain epitope integrity and promote optimal antigen processing and presentation, specific linkers were strategically selected based on their established immunological roles. CTL epitopes were joined using the AAY linker, which enhances proteasomal cleavage and facilitates efficient MHC class I presentation. HTL epitopes were connected using the GPGPG linker [18], commonly employed to preserve epitope conformation and improve MHC class II processing. B-cell epitopes were linked using KK linkers [18], which provide flexibility and enhance surface accessibility of antigenic regions. An immunostimulatory adjuvant was positioned at the N-terminus of the construct and connected to the epitope assembly via the EAAAK linker . This rigid α-helical linker provides structural stability and spatial separation between the adjuvant and epitope domains, thereby minimizing steric interference and enhancing overall immunogenicity [19]. All protein sequences used for epitope selection and vaccine construction were retrieved from public databases, and their corresponding accession numbers are provided in the Methods section to ensure transparency and reproducibility. Terminology related to epitopes, linkers, immune cell types, and vaccine platforms has been standardized throughout the manuscript for consistency.

### 2.7 Physicochemical and Solubility Analysis

The Expasy-ProtParam (https://web.expasy.org/protparam/) [20] web server was employed to assess key physicochemical attributes of these vaccine constructs, such as molecular mass, theoretical pI, half-life, aliphatic index, and grand average of hydropathicity. For antigenicity, the VaxiJen v2.0 server was used by a threshold of 0.4 for bacterial antigens, providing an accuracy range of 70-89%. ANTIGENpro (http://scratch.proteomics.ics.uci.edu/) [21], a sequence-based tool, was also applied to validate antigenicity further. Additionally, the SOLpro server (http://scratch.proteomics.ics.uci.edu/) [22], utilizing support vector machine architecture, predicted protein solubility when overexpressed in E. coli. Finally, allergenicity of the construct was assessed using AllerTOP v2.0, which boasts an accuracy of 88.7%.

### 2.8 Disulfide Engineering Strengthening Vaccine Constructs for Superior Stability

Disulfide engineering is a powerful technique employed in protein engineering to boost the stability, functionality, or specificity of proteins by introducing covalent disulfide bonds [23]. The designed vaccine constructs were submitted to

Disulfide by Design 2, an online server, for disulfide bond engineering analysis (http://cptweb.cpt.wayne.edu/DbD2/) [24], used to detect residues pairing with mutational potential essential for disulfide engineering. Computational modeling and mutational analyses guided the selection of optimal cysteine residue pairs [25], ensuring proper folding and minimal impact on protein activity. This approach not only enhanced the structural integrity of our constructs but also allowed us to probe functional mechanisms more effectively.

### 2.9 Structure Determination and Validation

To map optimal epitope locations, secondary structure prediction was performed using PSIPRED v4.0 (http://bioinf.cs.ucl.ac.uk/psipred/) [26] which analyzes α-helices, β-sheets, and coil regions through neural network- and information theory-based methods [25]. To gain insight into the vaccine's tertiary structure, the AlphaFold server (https://alphafold.ebi.ac.uk/) was employed [27], which is AI powered and uses a template-based approach and ranks structural models by P values.

Enhancement of the initial 3D structure was achieved with the GalaxyRefine web server (https://galaxy.seoklab.org/cgi-bin/submit.cgi?type=REFINE) [28], which applies molecular dynamics for iterative reassembling and structural optimization. For structural validation, we analyzed the Ramachandran plot with PROCHECK (https://servicesn.mbi.ucla.edu/PROCHECK/) and ProSA-web (https://prosa.services.came.sbg.ac.at/prosa.php) [29], confirming stereochemical quality and detecting any potential errors. Lastly, the refined 3D model of the vaccine construct was envisioned with Chimera 1.17.1 (https://www.cgl.ucsf.edu/chimera/) [30] for enhanced structural clarity.

### 2.10 Molecular Docking

Molecular docking was accompanied to forecast binding communications and affinities among the vaccine construct and immune receptors, aiding in understanding the potential immune response. The ClusPro 2.0 (https://cluspro.bu.edu/) docking, the balanced scoring mode was selected, which combines electrostatic, hydrophobic, and van der Waals interactions to generate optimal docking conformations. A total of 1000 rigid-body docking models were generated, which were subsequently clustered based on pairwise RMSD with a clustering radius of 9 Å. The top-ranked clusters were selected according to lowest weighted energy scores and cluster size. The selected docked complexes were then submitted to HADDOCK (https://wenmr.science.uu.nl/haddock2.4/) for semi-flexible refinement. In HADDOCK, active and passive residues were automatically defined, and docking was performed through the standard three-stage protocol: (i) rigid-body energy minimization (it0), (ii) semi-flexible simulated annealing (it1), and (iii) explicit solvent refinement (water refinement stage). The final docking solutions were ranked based on the HADDOCK score, which integrates van der Waals energy, electrostatic energy, desolvation energy, and restraint violation energy [31,32], including TLR2 (PDB ID: 4G8A), TLR4 (PDB ID: 4G8A), and TLR8 (PDB ID: 3W3G). After the docking results, the complex with TLR4 (V3-TLR4) was selected for further analysis due to its favorable global docking score and binding energy, indicating a strong potential for interaction.

### 2.11 iMODS-Based Structural Dynamics Analysis

The structural dynamics and strength of the prioritized vaccine complex were studied using iMODS (http://imods.chaconlab.org/) [33], which performs NMA based on an elastic network model. The PDB structure of the docked complex was uploaded in default format, and simulations were carried out using Cα atoms to assess collective molecular motions near equilibrium. The analysis generated deformability plots, eigenvalue spectra, B-factor profiles, variance maps, covariance matrices, and elastic network models, providing a comprehensive evaluation of molecular flexibility and rigidity. The eigenvalue, which reflects the energy required to deform the structure, was used as a key indicator of complex stability, where lower eigenvalues correspond to higher structural stability. Additionally, deformability and B-factor plots were analyzed to identify flexible hinge regions and structurally rigid domains critical for receptor binding. The covariance matrix was used to examine correlated, uncorrelated, and anti-correlated motions between residue pairs, while the elastic network model illustrated the stiffness distribution across the complex. These parameters collectively provided insight into the intrinsic motions, structural resilience, and binding stability of the vaccine-receptor complex [34], supporting its suitability for effective immune activation.

### 2.12 mRNA Construction and Codon Optimization

saRNA platform was selected for vaccine development due to its ability to achieve prolonged and robust antigen expression at substantially lower RNA doses compared with conventional non-replicating mRNA vaccines. Unlike standard mRNA, saRNA encodes a viral replicase complex that enables intracellular RNA amplification, thereby enhancing translational efficiency, sustaining antigen production, and improving immune stimulation–features particularly advantageous for multiepitope vaccine constructs [35]. The saRNA construct was designed based on an alphavirus-derived replicon backbone encoding the non-structural proteins nsP1-nsP4, which collectively mediate RNA replication. Specifically, nsP1 is

responsible for RNA capping and membrane association, nsP2 functions as a helicase and protease, nsP3 contributes to replication complex assembly, and nsP4 acts as the RNA-dependent RNA polymerase [36]. Together, these components enable autonomous RNA replication within host cells while lacking structural viral genes, ensuring biosafety [37]. The multi-epitope antigen cassette was inserted downstream of the subgenomic promoter, allowing efficient transcription and translation of the vaccine antigen without disrupting replicase function. To evaluate RNA folding stability and structural integrity, secondary structure prediction of the saRNA vaccine sequence was performed using the RNAfold server (https://rna.tbi.univie.ac.at/cgi-bin/RNAWebSuite/RNAfold.cgi) [38], which predicts RNA structures based on minimum free energy (MFE) calculations. The resulting MFE models provided insight into thermodynamic stability, revealing favorable folding patterns with stable base-pairing and limited structural constraints that could impede ribosomal access. These features are essential for efficient translation and sustained antigen expression and contribute to the overall effectiveness of the saRNA vaccine [39]. For optimal expression in a prokaryotic system during cloning and validation steps, codon optimization was performed using the integrated DNA technologies Codon Optimization Tool (https://www.idtdna.com/CodonOpt) [40]. The nucleotide sequence was adapted to match Escherichia coli codon usage preferences while maintaining the original amino acid sequence. This optimization ensured favorable GC content and a high codon adaptation index (CAI), supporting efficient transcription and translation during plasmid amplification and downstream experimental workflows. A schematic representation of the saRNA construct, illustrating the replicon backbone (nsP1-nsP4), subgenomic promoter, antigen cassette, untranslated regions, and regulatory elements, has been added to the manuscript to improve conceptual clarity and facilitate understanding of the vaccine architecture [41].

### 2.13 Host-Immune System Simulation

The immunogenic potential of the designed vaccine construct was evaluated using the C-ImmSim server (https://kraken.iac.rm.cnr.it/C-IMMSIM/) [42] which simulates mammalian immune system responses based on position-specific scoring matrices and machine learning algorithms [43]. This platform enables the computational assessment of both humoral and cellular immune dynamics following antigen exposure. To mimic a realistic vaccination regimen, the immune simulation was performed using three vaccine doses administered at four-week intervals, corresponding to simulation time steps 1, 84, and 168, respectively. The simulation volume was set to 50, and the total simulation duration was 1000-time steps to capture primary, secondary, and tertiary immune responses. A fixed random seed (13.461) was applied to ensure reproducibility of the stochastic simulation outputs. The resulting profiles of immunoglobulin production, immune cell populations, and cytokine responses were subsequently analyzed to assess the strength, durability, and quality of the vaccine-induced immune response.

## 3. Results and Discussions

### 3.1 Protein Sequence Retrieval

In this study, four immunogenic proteins from HHV-6 (Uganda-1102 strain) were selected for potential use in vaccine development. These proteins were retrieved from the UniProt database, monitored through detailed analyses of their immunogenicity and physicochemical properties. Based on antigenicity scores, the selected proteins included: Probable Envelope Glycoprotein B (antigenic score: 0.4799), Envelope glycoprotein L (antigenic score: 0.4432), Envelope glycoprotein H (antigenic score: 0.5284), and Major capsid protein (antigenic score: 0.4414).

Each protein underwent allergenicity evaluation using the AllergenFP v1.0 server, confirming a non-allergenic summary for all candidates (Table 1). Non-homology counter to the host proteome was also verified, ensuring the selected proteins had no similarity with host proteins using BLASTp software minimizing potential cross-reactivity [44]. Based on these assessments, the selected proteins proceeded to further analysis, guiding the deliberate development of a multi-epitope vaccine.

**Table 1.** Antigenicity and allergenicity assessment of the nominated proteins.

| Proteins Name | Antigen Score | Allergenicity Score |
|---|---|---|
| Envelope glycoprotein B | 0.4799 | NON-ALLERGEN |
| Envelope glycoprotein L | 0.4432 | NON-ALLERGEN |
| Envelope glycoprotein H | 0.5284 | NON-ALLERGEN |
| Major capsid protein | 0.4414 | NON-ALLERGEN |

### 3.2 B-cell Epitopes Prediction

For designing vaccine constructs that closely mimics the natural immune response and builds lasting adaptive immunity [45], specific epitopes were identified from each of the four target proteins using the ABCpred server. B-cell epitopes are important in triggering adaptive immunity [46], as they are renowned by B-cell receptors, leading to the construction of antibodies. To ensure strong immunogenicity, three top-scoring B-cell epitopes with a 16-mer window length were chosen from to each protein, the selection criteria was particularly antigenic, non-allergen and non-toxic (see Table 2). This selection aims to enhance the vaccine's effectiveness by carefully targeting epitopes that play a pivotal role in immune response.

### 3.3 Cytotoxic T Lymphocytes Epitopes Prediction

Cytotoxic T Lymphocytes (CTLs) are essential for activating the immune response. Their role in vaccine design is particularly valuable, as CTLs allow MHC class I molecules to present small peptide fragments on the surface of T-cells after treating [47]. This process is crucial for targeting infected cells and initiating a robust immune defense. To identify potential CTL epitopes for each protein sequence, the NetCTL 1.2 server was used, which evaluates each predicted epitope and assigns a score based on binding affinity and sensitivity. High-scoring epitopes indicate strong binding to MHC class I molecules and minimal sensitivity, indicating their potential to elicit a healthy immune response. From the four target proteins, a total of eight CTL peptides with the highest scores were selected based on antigenicity, non-allergenicity, and non-toxicity (Table 2).

### 3.4 Helper T-cells Prediction

Helper T-cells play a fundamental part in activating and sustaining adaptive immunity. They aid in the production and release of antibodies by B-cells and enhance the function of CTLs in targeting and eliminating infected cells [49]. Recognizing their importance in coordinating immune responses, The analysis focused on identifying HTL epitopes that complement B-cell and CTL responses to stimulate a well-rounded and potent immune response. The top two HTL epitopes were selected based on their lowest percentile rankings [50], reflecting strong binding affinities and immune-stimulating potential (Table 2). The selected epitopes were further passed from antigenicity, allergenicity and toxicity tests for their safety and immunogenic properties. Results confirmed that all chosen HTL epitopes are non-allergenic, non-toxic, antigenic, which is crucial for a robust immune response.

**Table 2.** Top prioritized B-cell epitope, HTL-epitopes and CTL-epitopes and their antigenicity, allergenicity and toxicity scores.

| Epitopes | Antigenicity Score | Allergenicity Score | Toxicity Score |
|---|---|---|---|
| NTLNLFPLNFKSITNK | 1.0783 | NON-ALLERGEN | Non-Toxin |
| HKYPFRICISAKGTDL | 0.6778 | NON-ALLERGEN | Non-Toxin |
| VELPEGLYCPRTEINL | 0.5323 | NON-ALLERGEN | Non-Toxin |
| KLPFRSSRPTILIRNT | 0.9880 | NON-ALLERGEN | Non-Toxin |
| YSTKNTGPMPVLRVLK | 0.5038 | NON-ALLERGEN | Non-Toxin |
| LQNIYEKHMFFTNLTF | 0.8352 | NON-ALLERGEN | Non-Toxin |
| AKDIATTYNFTQHLSF | 0.6901 | NON-ALLERGEN | Non-Toxin |
| VSLIRLVKRTISISNL | 0.7511 | NON-ALLERGEN | Non-Toxin |
| NLFLPLNFSITNKRKF | 1.2507 | NON-ALLERGEN | Non-Toxin |
| HYIRAGYNHKYPFRRI | 1.1044 | NON-ALLERGEN | Non-Toxin |
| ENTDSFYSNIGFILLY | 0.7771 | NON-ALLERGEN | Non-Toxin |
| KLPFRSSRPTILIRN | 0.8955 | NON-ALLERGEN | Non-Toxin |
| PMNDILRLSPVPSVK | 0.8055 | NON-ALLERGEN | Non-Toxin |
| GPLQYIYIKNIDELK | 0.5949 | NON-ALLERGEN | Non-Toxin |
| DIATTYNFTQHLSFV | 0.9254 | NON-ALLERGEN | Non-Toxin |
| AAAFAHYRNLVSLIRL | 0.5528 | NON-ALLERGEN | Non-Toxin |
| TLNLFPLNF | 1.5023 | NON-ALLERGEN | Non-Toxin |
| AKAKYPFSY | 0.6997 | NON-ALLERGEN | Non-Toxin |
| YSNIGFILLY | 1.6602 | NON-ALLERGEN | Non-Toxin |
| SSRPTILIR | 0.9319 | NON-ALLERGEN | Non-Toxin |
| RLSPVPSVK | 2.1086 | NON-ALLERGEN | Non-Toxin |
| IYIKNIDEL | 0.9366 | NON-ALLERGEN | Non-Toxin |
| EAKDIATTY | 0.9728 | NON-ALLERGEN | Non-Toxin |
| AHYRNLVSL | 0.8009 | NON-ALLERGEN | Non-Toxin |

### 3.5 Assembling Epitopes for Vaccine Constructs

For the vaccine constructs, eight CTL epitopes, eight HTL epitopes, and eight B-cell epitopes were strategically assembled into a single linear sequence. These components were connected using the EAAAK linker, which is recognized for its structural stability and ability to provide spatial separation between the adjuvant and epitope regions [51], facilitating efficient immune activation. To design the chimeric HHV-6 vaccine models, CTL, HTL, and B-lymphocyte epitopes was cherished by particular amino acid linkers–'GGGS' 'HEYGAEALERAG' and 'EAAAK', respectively [52]. To augment immunogenicity, four distinct adjuvants–β-defensin, conserved HBHA, ribosomal protein, and HBHA–were integrated at the N-terminus of the vaccine construct and linked using an EAAAK linker to ensure structural stability and functional separation. To further enhance vaccine potency, expression efficiency, bioactivity, and overall immunogenic response, the pan-DR epitope (PADRE; AKVAAWTLKAAAC) was incorporated. This epitope is well known for its ability to promote $CD4^+$ T-cell activation and broad HTL responses (Supplementary Table 1).

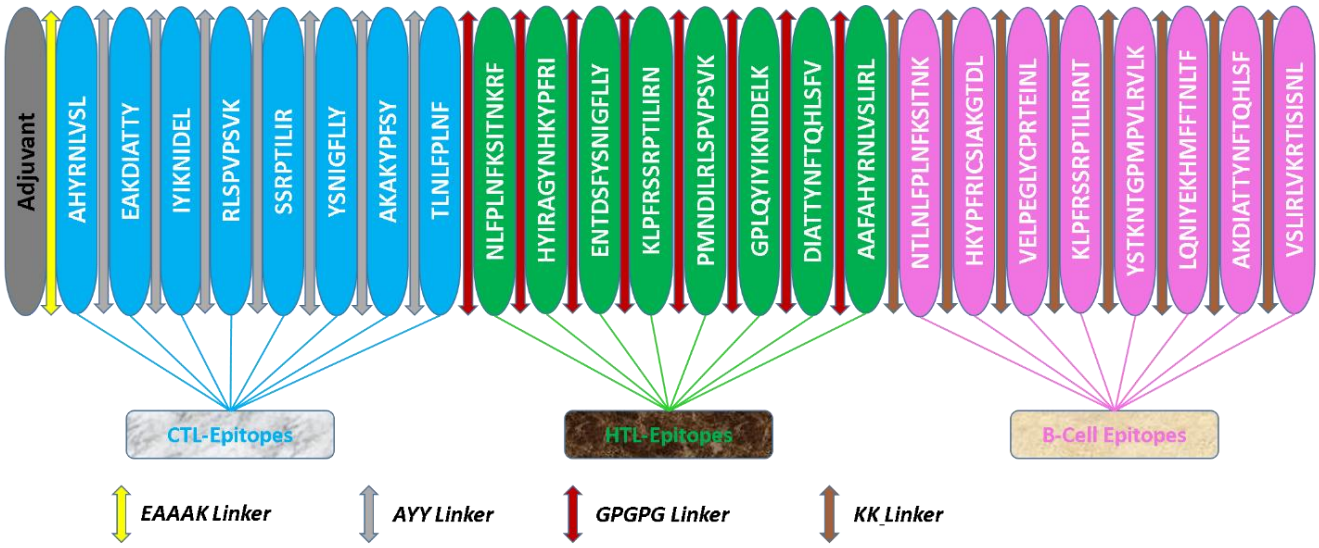


**Figure 2.** The multi epitope V3 construction through linkers and adjuvants.

### 3.6 Physiochemical Chemical Assessment of Constructs

To evaluate the physicochemical properties of the vaccine constructs, including stability, solubility, and overall suitability for subsequent experimental phases [53], the constructs were analyzed using the ExPASy ProtParam online server [54], the physicochemical outputs from Expasy, like molecular weight, isoelectric point (pI), extinction coefficient, and instability index, provide essential comprehensions keen on the biochemical properties of proteins. These results are fundamental for understanding protein behavior, stability, and solubility under various conditions. This comprehensive approach to vaccine construction aims to create a stable and effective candidate, ready for subsequent *in vivo* validation (Table 3).

**Table 3.** Physiochemical properties of vaccine constructs.

| Vaccine Construct | HHV6 - V1 | HHV6 - V2 | HHV6 - V3 | HHV6 - V4 |
|---|---|---|---|---|
| No. of Amino Acids | 622 | 508 | 613 | 593 |
| Molecular Weight (kDa) | 69.46 | 56.99 | 68.34 | 65.27 |
| Theoretical pI | 9.77 | 10.05 | 9.73 | 9.73 |
| Aliphatic Index | 83.91 | 80.18 | 85.6 | 86.64 |
| Grand Average of Hydropathicity | -0.366 | -0.355 | -0.348 | -0.212 |
| Instability Index | 40.8 | 40.17 | 37.42 | 35.44 |
| GC Content (%) | 72.64 | 74.21 | 73.44 | 72.75 |
| CAI | 0.94 | 0.9 | 0.93 | 0.97 |
| Antigenicity (VaxiJen v2.0, threshold = 0.4) | 0.6842 (Antigenic) | 0.7289 (Antigenic) | 0.6838 (Antigenic) | 0.6706 (Antigenic) |
| Allergenicity (AllerTOP v2.0) | Non-allergen | Non-allergen | Non-allergen | Non-allergen |

### 3.7 Secondary Structure Prediction

The secondary structure of the vaccine construct was predicted through the PSIPRED server [55], a reliable tool for analyzing protein sequences. PSIPRED utilizes position-specific scoring matrices to forecast alpha-helices, beta-strands, and random coil regions within the protein (Figure 3 and figure S1, S2, S3). These analyses was executed to realize the structural composition of the vaccine and assess its folding patterns, which are critical for maintaining functionality and stability. The results revealed a well-balanced distribution of alpha-helices and beta-strands, essential for providing structural integrity, along with coil regions contributing to flexibility [56]. These findings helped validate the structural design and supported further analyses for vaccine optimization.

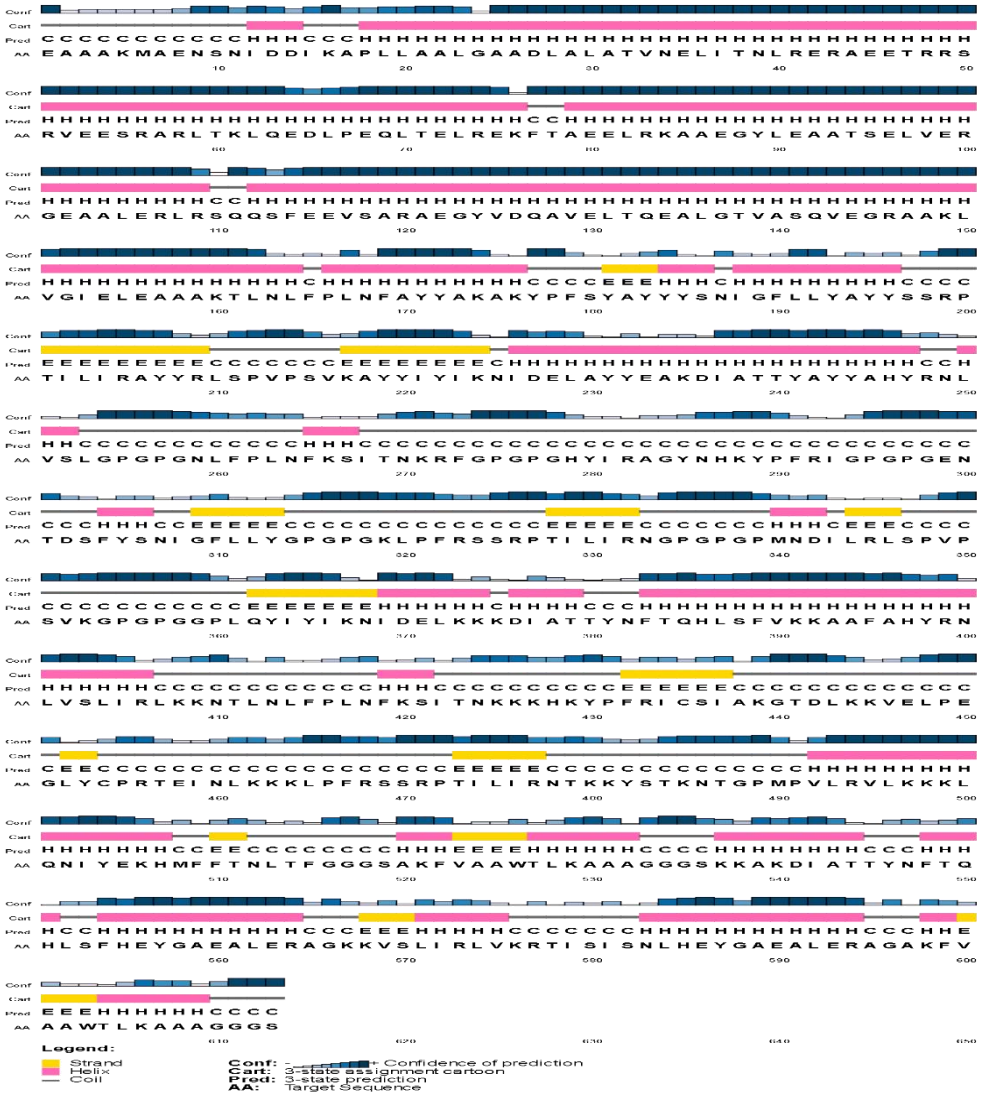


**Figure 3.** 2D structure of V3 construct, yellow color in the structure represents beta strands, the pinks color represents Alpha Helix and the black represents random coils in the structure.

### 3.8 D structure Evaluation and Prediction

Ensuring a robust 3D structure for the chimeric vaccine constructs, the Alphafold server [57] generated initial models (Figure 4A), refined further using the GalaxyRefine server (Figure 4B). After producing four refined models, the most optimal one was chosen based on high GDT-HA scores and favorable Rama-favored ratings (Table S1). The ProSA-web Z-score for the top-prioritized HHV-6 construct V3 stood at -2.02 confirming its stability and reliability (Figures 4C) Validation via the Ramachandran plot demonstrated that 95.36%, 88.88%, 97.5% and 81.9% of residues in the V1, V2, V3 and V4 constructs respectively were within the most favored regions, reflecting quality across all models (Figure 4D). The remaining vaccine constructs V1, V2 and V4 figures are available in supplementary file as (Figure S4, S5, S6).

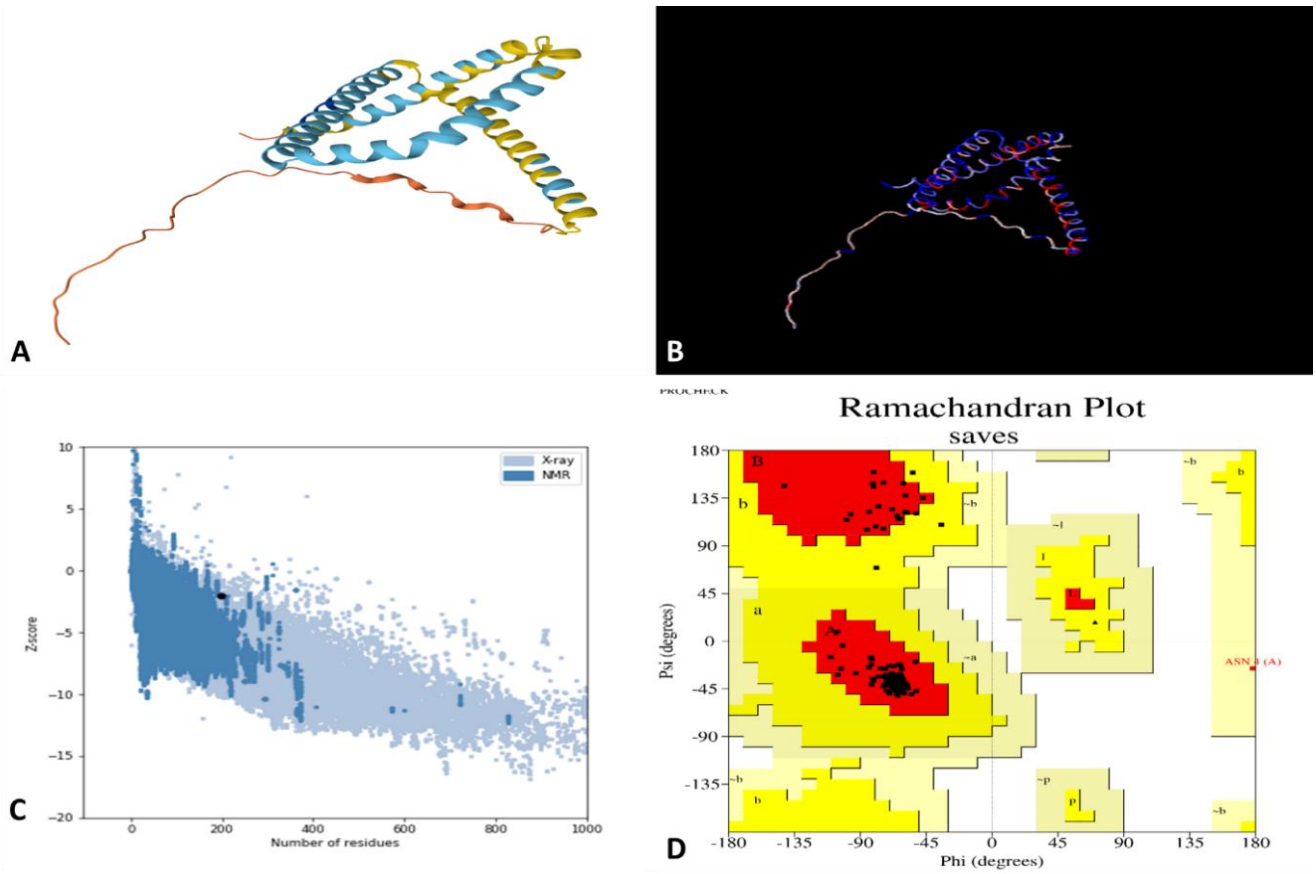


**Figure 4.** Vaccine construct V3. (A) 3D structure predicted on Alphafold server. (B) validated structure of V3. (C) Z-score of V3 construct. (D) ramachandran plot of V3 construct scoring 97.5% of residues in most favored region, 1.9% of residues in additional allowed region, 0.6% in generously allowed region and 0% in disallowed regions.

### 3.9 Molecular Docking Analysis

Molecular docking was executed to calculate the binding affinity and interaction of four vaccine constructs (V1, V2, V3, and V4) with Toll-like receptors TLR2, TLR4, and TLR8, aiming to assess their potential for eliciting immune responses. The purpose was to identify the construct that demonstrated the strongest and most stable binding to these receptors, as effective receptor engagement is crucial for activating innate immunity [58], the docked score of all constructs with receptors are in (Table 4).

**Table 4.** Docking results of all vaccine constructs with toll like receptors.

| Ligands vs Receptors | Docking Score | Confidence Score | Lowest Binding Energy | Ligand RMSD (Å) | Docked Models |
|---|---|---|---|---|---|
| V1-TLR2 | -305.4 | 0.9572 | -1260.9 | 105.46 | M3 |
| V1-TLR4 | -336.18 | 0.9764 | -1394.9 | 43.04 | M1 |
| V1-TLR8 | -284.13 | 0.936 | -1345.4 | 51.35 | M1 |
| V2-TLR2 | -293.23 | 0.9461 | -1786.3 | 147.18 | M1 |
| V2-TLR4 | -298.19 | 0.9509 | -1247 | 28.92 | M0 |
| V2-TLR8 | -297.73 | 0.9505 | -1539.2 | 70.45 | M1 |
| V3-TLR2 | -343.61 | 0.9796 | -1293.2 | 143.52 | M0 |
| V3-TLR4 | -361.46 | 0.9856 | -1302.2 | 61.11 | M0 |
| V3-TLR8 | -345.36 | 0.9803 | -1552.3 | 94.78 | M1 |
| V4-TLR2 | -194.54 | 0.7091 | -1113.2 | 171.88 | M5 |
| V4-TLR4 | -219.25 | 0.7998 | -904.8 | 33.88 | M4 |
| V4-TLR8 | -233.11 | 0.8405 | -1222.3 | 85.4 | M4 |

The top prioritized construct on the basis of lowest binding energy and docking score was further submitted to HADDOCK server [59] to evaluate the interaction stability, and the count of important interactions, including hydrogen bonds and hydrophobic interactions (Table 5). Among the constructs, V3 exhibited the most favorable binding affinity and interactions with all three receptors, particularly TLR4, suggesting its superiority in receptor activation and immunogenic potential (Figure 5). This analysis provided valuable insights for selecting the most promising vaccine candidate for further validation.

**Table 5.** The HADDOCK score of top prioritized vaccine construct V3-TLR4.

| Parameter | HHV6-V3-TLR4 |
|---|---|
| Cluster Number | 0 |
| HADDOCK Score | -5.3 +/- 4.1 |
| Cluster Size | 6 |
| RMSD from Lowest-Energy Structure | 11.3 +/- 0.9 Å |
| Van der Waals Energy | -72.7 +/- 9.2 kcal/mol |
| Electrostatic Energy | -399.8 +/- 16.3 kcal/mol |
| Desolvation Energy | 19.2 +/- 3.9 kcal/mol |
| Z-Score | -2.02 |

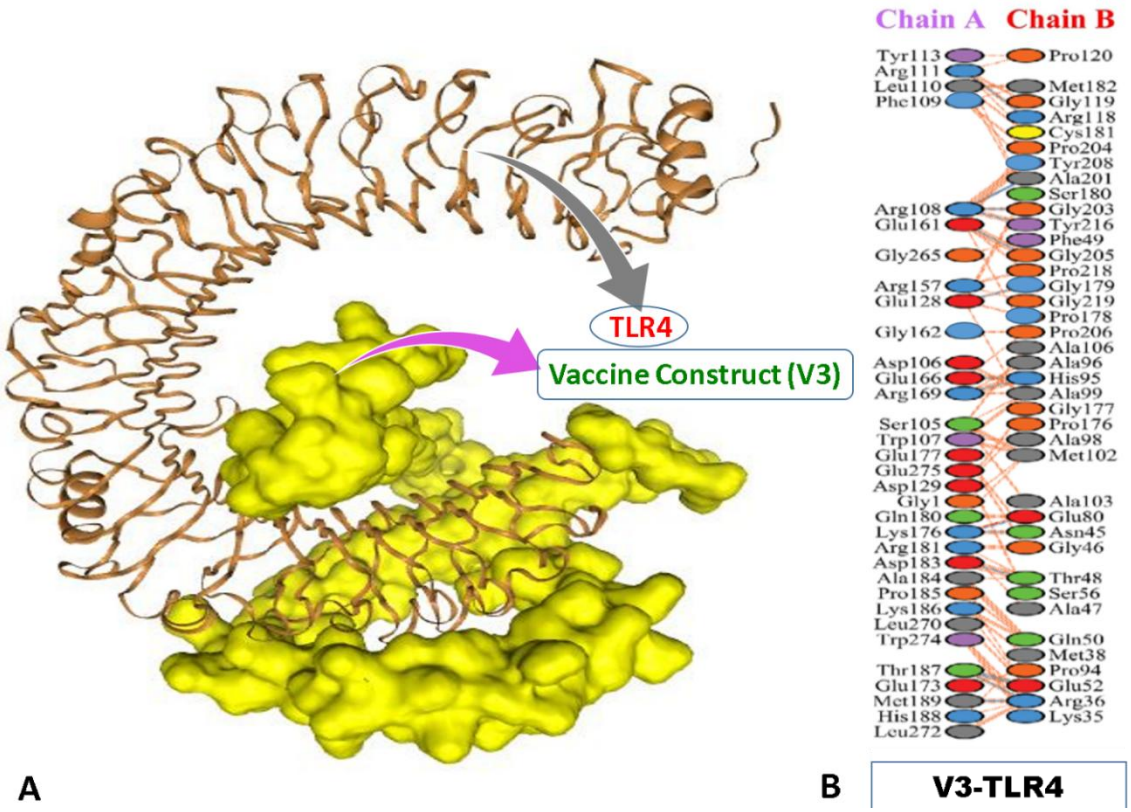


**Figure 5.** Docked structure of MEV and TLR receptor. (A) Docked structure of vaccine construct V3-TLR4. (B) Salt bridge between V3 and TLR4.

### 3.10 Dynamic Stability Analysis of Vaccine Complex

iMODS analysis was employed in our prioritized vaccine complex to estimate the structural dynamics and stability of the V3-TLR4 complex. This tool provided critical insights into the flexibility and large-scale motions of the complex, crucial for ensuring its efficient interaction with immune receptors [60]. The analysis generated deformation energy graphs, which highlighted the regions prone to structural instability, and eigenvalue plots, which quantified the energy essential for deformation, reflecting the overall rigidity of the complex. Additionally, B-factor and mobility graphs revealed the flexible and rigid regions, aiding in optimizing the construct for better immunogenicity and receptor binding.

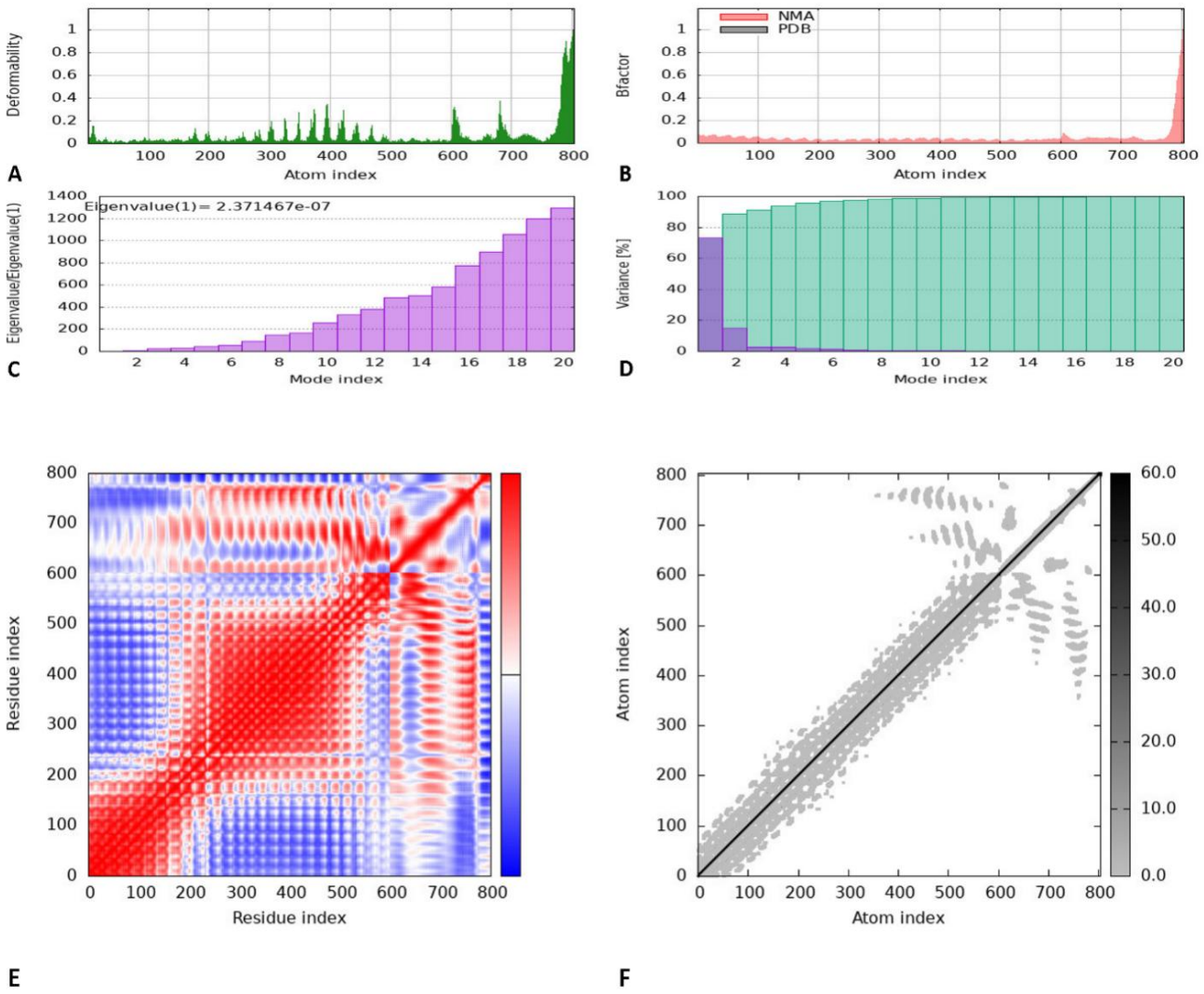


**Figure 6.** Results of iMODS of vaccine V3-TLR4 docking complex. (A) Deformability plot. (B) B-factor of complex V3-TLR4. (C) Eigenvalue of the complex. (D) Variance of complex V3-TLR4. (E) Covariance matrix analysis of complex V3-TLR4. (F) Elastic network model of complex V3-TLR4.

### 3.11 mRNA Vaccine Construction and Codon Optimization

Additionally, for the saRNA vaccine construct, secondary structure prediction of the ranked vaccine mRNA sequence was performed using two online servers, Mfold v2.3 [61], and the RNAfold tool from the ViennaRNA [62] webserver was employed. Inauguration predictions on centroid outranked structure and defining the MFE through the inventive McCaskill's algorithm., shedding light on the structural dynamics crucial for vaccine effectiveness. The primary output, the MFE (ΔG in Kcal/mol), indicates the constancy of the mRNA folding structure, with lower values signifying greater stability (Figure 7). The nucleotide sequence for the multi-epitope vaccine was optimized using the ExpOptimizer tool [63], selecting “Escherichia coli” as the expression host. After optimization, using integrated DNA technologies server [64] the CAI improved to 0.9, which falls within the preferred range of 0.8 to 1.0. Additionally, the GC content was fine-tuned to 50.71%, aligning well with the ideal range of 40% to 60%, ensuring efficient expression and stability.

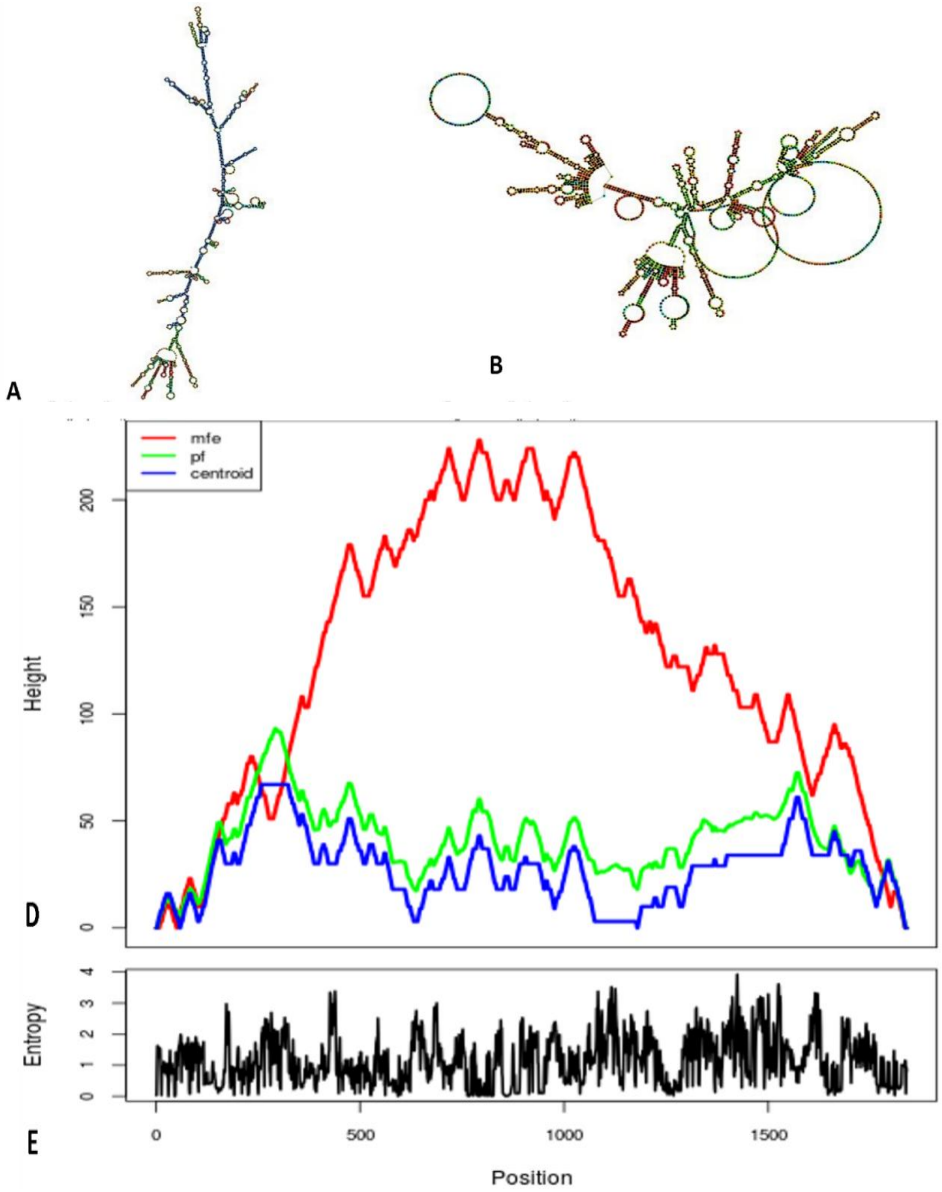


**Figure 7.** mRNA vaccine secondary structure of MEV. (A) The model performance analysis of the MFE of the HHV6 V3-TLR4 mRNA structure highlights its thermodynamic stability, providing insights into its efficient folding and functional potential. (B) The projected model of the secondary centroid structure further illustrates the MFE configuration, representing the most thermodynamically favorable conformation of the HHV6 V3-TLR4 mRNA. (C) The mountain plot visualization integrates the MFE structure, thermodynamic ensemble, and centroid structure, offering a comprehensive understanding of the mRNA's stability and secondary structure interactions. (D) The positional entropy plot reveals the variability and flexibility at specific sites, providing critical information on structural robustness and the dynamic adaptability of the mRNA.

### 3.12 Immune Simulation

The *in silico* immune simulation was performed using the C-ImmSim server to evaluate the immunogenic potential of the designed HHV-6 multi-epitope saRNA vaccine. The simulation outcomes demonstrate a coordinated activation of humoral and cellular immune responses, as shown in the graph (Figure 8).

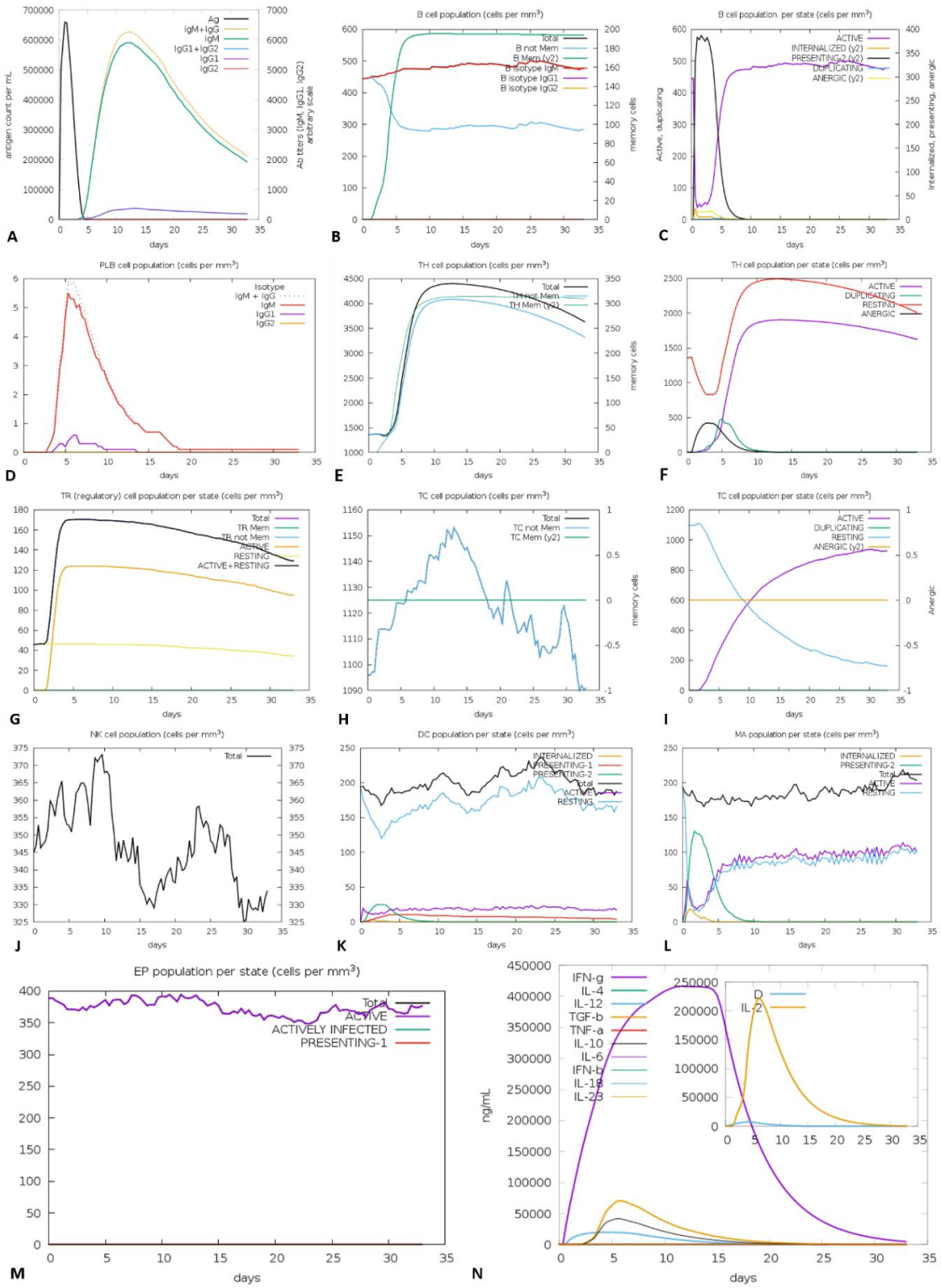


**Figure 8.** The *in silico* immune simulation results of the vaccine construct, obtained using C-ImmSim, are summarized as follows: (A) Following stimulation with a multiepitope vaccine, immunoglobulin levels were assessed. (B) Memory B-lymphocyte levels (y2) were quantified, and immunoglobulin isotypes (IgM, IgG1, IgG2) were analyzed during the immune response. (C) The counts of active, proliferative, quiescent, and anergic B-lymphocytes were evaluated alongside (D) the plasma cell populations under various conditions. (E) Total and memory T-lymphocyte populations were examined. (F) The numbers of active, proliferative, quiescent, and anergic T-lymphocytes were measured. (G) The distribution of various T-lymphocyte subsets was assessed. (H) T-lymphocyte populations were evaluated across different conditions. (I) Counts of active, proliferative, quiescent, and anergic T-lymphocytes were analyzed. (J) The total number of NK cells was determined. (K) The volume of dendritic cells (DCs) was measured. (L) The number of macrophages was calculated. (M) Eosinophil counts were determined. (N) Cytokines produced during the immune response were quantified.

Following antigen administration, a strong primary immune response was observed, characterized by a rapid increase in antigen concentration and an early rise in IgM antibodies, beginning approximately 5-7 days post-immunization (Figure 8A). This initial IgM surge reflects the first line of adaptive immune defense upon exposure to the HHV-6 antigen. Subsequently, a pronounced secondary immune response was evident, marked by a substantial increase in IgG isotypes (IgG1 and IgG2) along with sustained IgM levels, indicating effective class switching and affinity maturation. The elevated IgG titers suggest enhanced immunological memory and improved antigen-specific neutralization capacity upon repeated antigen exposure (Figure 8A). Consistent with these observations, B-cell populations showed marked expansion. Total B-cell counts increased rapidly during the secondary phase, accompanied by the generation of memory B cells (Figure 8B). The distribution of B-cell states revealed a transient rise in actively proliferating B cells, followed by stabilization into memory and resting phenotypes, indicating successful establishment of long-term humoral immunity (Figure 8C-D). The vaccine construct also elicited a robust T-cell-mediated immune response. Both helper T (Th) and cytotoxic T (Tc) cell populations expanded significantly following immunization (Figure 8E). The early activation and proliferation of Th cells support efficient antigen presentation and B-cell help, while the expansion of Tc cells indicates the potential for effective clearance of HHV-6-infected cells. Analysis of T-cell functional states showed a clear transition from active and proliferating cells during the early immune phase to resting and memory states at later time points (Figure 8F-I). The presence of memory Th and Tc cells highlights the capacity of the vaccine to induce durable cellular immune memory, which is critical for long-term protection against viral reactivation. Innate immune components were also strongly activated following vaccination. Natural killer (NK) cell populations increased rapidly, peaking around day 5 post-immunization (approximately 370-375 cells/mm$^3$), before stabilizing with moderate fluctuations over time (Figure 8J) . This early NK-cell activation likely contributes to initial viral control and supports the development of adaptive immunity. Similarly, dendritic cells (DCs) showed a notable increase, with resting DCs constituting the majority of the population (Figure 8K). The rise in resting DCs following antigen exposure indicates efficient antigen uptake and processing, while the limited number of presenting DC subsets suggests controlled and sustained immune activation rather than excessive inflammation. Macrophage populations also increased steadily, reflecting their role in antigen presentation and cytokine production (Figure 8L). The simulation further demonstrated stable effector cell (EP) populations, with active and presenting effector states maintained throughout the simulation period (Figure 8M). This supports the persistence of immune surveillance mechanisms following vaccination. Cytokine profiling revealed elevated levels of IFN-γ and IL-2, which are hallmark cytokines of a Th1-biased immune response (Figure 8N). IFN-γ plays a critical role in antiviral defense by enhancing macrophage activation and cytotoxic T-cell function, while IL-2 supports T-cell proliferation and memory formation. Additional cytokines, including IL-12 and TNF-α, further indicate coordinated innate-adaptive immune crosstalk. Collectively, the immune simulation results demonstrate that the HHV-6 multi-epitope saRNA vaccine is capable of inducing strong primary and secondary immune responses, effective immunoglobulin class switching, robust B- and T-cell memory formation, and a favorable Th1-oriented cytokine profile. These findings suggest that the designed vaccine construct has the potential to provide comprehensive and long-lasting immune protection against HHV-6 infection and reactivation.

## 4. Discussion

The present study demonstrates a comprehensive immunoinformatics-driven framework for the rational design of a multiepitope saRNA vaccine targeting HHV-6, a ubiquitous virus with significant clinical relevance in immunocompromised individuals. Although HHV-6 infection is often asymptomatic in immunocompetent hosts, its capacity for latency, chromosomal integration, and reactivation is associated with severe neurological disorders, transplant rejection, and systemic complications. These features underscore the urgent need for prophylactic strategies beyond conventional antiviral therapies [18,65].

A key strength of this work lies in the systematic epitope prioritization strategy, which integrated B-cell, CTL, and HTL epitopes derived from structurally and immunologically relevant HHV-6 proteins. This multiepitope approach aligns with growing evidence that vaccines capable of activating both humoral and cellular immunity provide superior protection against persistent and latent viral infections compared with single-antigen formulations. Similar multiepitope strategies have shown enhanced immunogenicity in computational and experimental studies targeting herpesviruses and other DNA viruses, supporting the rationale of the present design. The incorporation of the 50S ribosomal L7/L12 adjuvant further strengthens the construct by promoting innate immune activation and antigen presentation. Previous studies have demonstrated that ribosomal protein-based adjuvants effectively enhance T-cell-mediated immunity and bias immune responses toward protective Th1 profiles [66]. The careful use of optimized linkers ensured appropriate spatial separation of epitopes, reducing the risk of junctional epitope formation and preserving antigen processing efficiency. Together, these design principles reflect current best practices in epitope-based vaccine engineering. Structural validation provided important mechanistic support for the vaccine's immunological potential. Accurate folding and conformational stability, predicted using AlphaFold and refined via GalaxyRefine, are critical determinants of antigen recognition and immune receptor engagement [67]. Improper protein folding can compromise epitope accessibility or trigger aberrant immune responses. The

favorable structural quality metrics observed here are consistent with recent reports demonstrating the reliability of AI-based structure prediction tools for vaccine design.

Interaction analyses with innate immune receptors revealed TLR4 as a dominant recognition partner, suggesting that the vaccine may effectively activate early innate immune signaling pathways. This observation is consistent with earlier findings showing that TLR4 engagement plays a pivotal role in antiviral immunity by promoting dendritic cell maturation, cytokine secretion, and subsequent adaptive immune activation [68]. NMA further indicated favorable conformational dynamics of the vaccine-TLR4 complex, suggesting stable receptor engagement under physiological conditions–an essential feature for efficient immune priming. From a translational perspective, the adoption of a saRNA platform represents a notable advancement over conventional non-replicating mRNA vaccines. saRNA systems enable prolonged antigen expression at significantly lower doses, thereby enhancing immunogenicity while potentially reducing manufacturing costs and reactogenicity. The inclusion of codon optimization and RNA secondary structure analysis further supports efficient expression and stability, consistent with recent saRNA vaccine studies targeting viral pathogens.

The immune simulation results provide theoretical evidence that the designed vaccine could induce a balanced and durable immune response, characterized by immunoglobulin class switching, memory B-cell formation, cytotoxic and HTL activation, and a Th1-skewed cytokine profile. Such immune characteristics are particularly important for controlling HHV-6, which employs immune evasion and latency mechanisms. Comparable immune profiles have been reported in computational studies of multiepitope vaccines against herpesviruses, reinforcing the validity of the predicted trends.

## 5. Study Limitations and Future Perspectives

Despite the promising findings presented in this study, several limitations should be acknowledged. First, the vaccine design and evaluation were conducted entirely using computational and immunoinformatics-based approaches. While these tools provide powerful and cost-effective insights into antigenicity, immunogenicity, structural stability, and immune interactions, they cannot fully replicate the complexity of biological systems. Consequently, the predicted immune responses, molecular interactions, and stability profiles require experimental validation. To address this limitation, a clear roadmap for future experimental validation is proposed. Initial validation should involve *in vitro* synthesis of the saRNA followed by lipid nanoparticle (LNP) encapsulation to ensure efficient cellular delivery and protection from degradation [65,66]. *In vitro* expression assays using mammalian cell lines should then be performed to confirm antigen expression, translational efficiency, and intracellular localization. Protein expression can be verified using techniques such as Western blotting, immunofluorescence, and Enzyme-Linked Immunosorbent Assay. Subsequently, *in vivo* validation in appropriate animal models is essential to evaluate vaccine immunogenicity, safety, and protective efficacy. These studies should assess humoral immune responses (IgM and IgG subclass production), cellular immune activation ($CD4^+$ and $CD8^+$ T-cell responses), cytokine profiles, and memory cell generation. Toxicity and biodistribution analyses will also be necessary to confirm the safety of the saRNA-LNP formulation. Where feasible, viral challenge studies may be conducted to evaluate protective efficacy against HHV-6 infection or reactivation.

Second, although immune simulations suggest robust humoral and cellular immune activation, actual host immune responses may vary due to genetic diversity, HLA polymorphism, and host-specific immunological factors. Additionally, the ability of HHV-6 to establish latency and integrate into the human genome poses unique biological challenges that cannot be fully addressed through computational modeling alone.

Future studies should also focus on optimizing vaccine delivery strategies, including LNP composition, dosing regimens, and booster schedules, as well as evaluating alternative adjuvant configurations to further enhance immunogenicity. Ultimately, clinical trials will be required to determine the safety, immunogenicity, and protective potential of the proposed vaccine in diverse human populations. Collectively, these efforts will be critical for translating the present *in silico* findings into a viable and effective prophylactic strategy against HHV-6 infection and reactivation.

## 6. Conclusion

In conclusion, this study determines the dynamic design as well as computational evaluation of a multiepitope mRNA vaccine targeting HHV-6, leveraging immunoinformatics and reverse vaccinology to address a critical unmet need. The vaccine construct, enriched with antigenic, non-allergenic, and non-toxic epitopes linked to an effective adjuvant, exhibited strong binding affinity and stability with immune receptors, as confirmed over molecular docking, dynamics simulations, and binding energy analyses. Immune simulations further validated its potential to stimulate a robust humoral and cellular immune response, laying a solid foundation for its prophylactic application. The iMODS analysis affirmed the structural flexibility and permanency of the vaccine-receptor complex, enhancing confidence in its functional viability. While these computational findings are promising, experimental validation will be crucial to confirm the vaccine's immunogenicity,

safety, and protective efficacy, ultimately paving the way for combating HHV-6 infections and reactivation in high-risk populations.

**Acknowledgements**

We are thankful to Abdul Wali Khan University for providing the best environment for this research.

**Ethics Statement**

Not Applicable.

**Data Availability Statement**

All Data are available in the online published article.

**Author Contributions**

Waseef Ullah have design, analyse and write the full manuscript.

**Conflicts of Interest**

There is no conflict of interest.

**Generative AI Statement**

The author declares that no Gen AI was used in the creation of this manuscript.

**References**

[1] Agut H, Bonnafous P, Gautheret-Dejean A. Laboratory and clinical aspects of human herpesvirus 6 infections. Clinical Microbiology Reviews, 2015, 28(2), 313-335. DOI: 10.1128/CMR.00122-14
[2] Eliassen E, Hemond CC, Santoro JD. HHV-6-associated neurological disease in children: Epidemiologic, clinical, diagnostic, and treatment considerations. Pediatric Neurology, 2020, 105, 10-20. DOI: 10.1016/j.pediatrneurol.2019.10.004
[3] Miao L, Zhang Y, Huang L. mRNA vaccine for cancer immunotherapy. Molecular Cance, 2021, 20(1), 41. DOI: 10.1186/s12943-021-01335-5
[4] Pardi N, Hogan MJ, Porter FW, Weissman D. mRNA vaccines–a new era in vaccinology. Nature Reviews Drug Discovery, 2018, 17(4), 261-279. DOI: 10.1038/nrd.2017.243
[5] Pardi N, Krammer F. mRNA vaccines for infectious diseases–advances, challenges and opportunities. Nature Reviews Drug Discovery, 2024, 1-24. DOI: 10.1038/s41573-024-01042-y
[6] Costa GL, Sautto GA. Exploring T-cell immunity to hepatitis C virus: Insights from different vaccine and antigen presentation strategies. Vaccines, 2024, 12(8), 890. DOI: 10.3390/vaccines12080890
[7] Consortium U. UniProt: A worldwide hub of protein knowledge. Nucleic Acids Research, 2019, 47(D1), D506-D515. DOI: 10.1093/nar/gky1049
[8] Doytchinova IA, Flower DR. VaxiJen: A server for prediction of protective antigens, tumour antigens and subunit vaccines. BMC Bioinformatics, 2007, 8(1), 1-7. DOI: 10.1186/1471-2105-8-4
[9] Dimitrov I, Bangov I, Flower DR, Doytchinova I. AllerTOP v. 2–a server for *in silico* prediction of allergens. Journal of Molecular Modeling, 2014, 20, 1-6. DOI: 10.1007/s00894-014-2278-5
[10] Mahram A, Herbordt MC. NCBI BLASTP on high-performance reconfigurable computing systems. ACM Transactions on Reconfigurable Technology and Systems, 2015, 7(4), 1-20. DOI: 10.1145/2629691
[11] Gu Y, Sun XM, Huang JJ, Zhan B, Zhu XP. A multiple antigen peptide vaccine containing $CD4^+$ T cell epitopes enhances humoral immunity against Trichinella spiralis infection in mice. Journal of Immunology Research, 2020, 2020(1), 2074803. DOI: 10.1155/2020/2074803
[12] Malik AA, Ojha SC, Schaduangrat N, Nantasenamat C. ABCpred: A webserver for the discovery of acetyl-and butyryl-cholinesterase inhibitors. Molecular Diversity, 2022, 467-487. DOI: 10.1007/s11030-021-10292-6
[13] Saha S, Raghava GPS. Prediction of continuous B-cell epitopes in an antigen using recurrent neural network. Proteins: Structure, Function, and Bioinformatics, 2006, 65(1), 40-48. DOI: 10.1002/prot.21078
[14] Saha S, Raghava GPS. Prediction methods for B-cell epitopes. Immunoinformatics Predict Immunogenicity Silico, 2007, 387-394. DOI: 10.1007/978-1-60327-118-9_29
[15] Vita R, Mahajan S, Overton JA, Dhanda SK, Martini S, Cantrell JR, et al. The immune epitope database (IEDB): 2018 update. Nucleic Acids Research, 2019, 47(D1), D339-D343. DOI: 10.1093/nar/gky1006
[16] Nielsen M, Justesen S, Lund O, Lundegaard C, Buus S. NetMHCIIpan-2.0-Improved pan-specific HLA-DR predictions using a

novel concurrent alignment and weight optimization training procedure. Immunome Research, 2010, 6, 9. DOI: 10.1186/1745-7580-6-9
[17] Rathore AS, Arora A, Choudhury SPS, Tijare P, Raghava GPS. ToxinPred 3.0: An improved method for predicting the toxicity of peptides. Computers in Biology and Medicine, 2024, 108926. DOI: 10.1016/j.compbiomed.2024.108926
[18] Bhattacharya M, Sharma AR, Ghosh P, Patra P, Patra BC, Lee SS, et al. Bioengineering of novel non-replicating mRNA (NRM) and self-amplifying mRNA (SAM) vaccine candidates against SARS-CoV-2 using immunoinformatics approach. Molecular Biotechnology, 2022, 64(5), 510-525. DOI: 10.1007/s12033-021-00432-6
[19] Waqas M, Aziz S, Bushra A, Halim SA, Ali A, Ullah S, et al. Employing an immunoinformatics approach revealed potent multi-epitope based subunit vaccine for lymphocytic choriomeningitis virus. Journal of Infection and Public Health, 2023, 16(2), 214-232. DOI: 10.1016/j.jiph.2022.12.023
[20] ExPASy BRP. ProtParam Tool. SIB Bioinforma Resour Portal. Availible at: https://www.expasy.org/protparam/ (accessed on October 2016).
[21] Smiline Girija AS. Delineating the immuno-dominant antigenic vaccine peptides against gacS-sensor kinase in *Acinetobacter baumannii*: An *in silico* investigational approach. Frontiers in Microbiology, 2020, 11, 2078. DOI: 10.3389/fmicb.2020.02078
[22] Magnan CN, Randall A, Baldi P. SOLpro: Accurate sequence-based prediction of protein solubility. Bioinformatic, 2009, 25(17), 2200-2207. DOI: 10.1093/bioinformatics/btp386
[23] Vardar-Yel N, Tütüncü HE, Sürmeli Y. Lipases for targeted industrial applications, focusing on the development of biotechnologically significant aspects: A comprehensive review of recent trends in protein engineering. International Journal of Biological Macromolecules, 2024, 273(Pt1), 132853. DOI: 10.1016/j.ijbiomac.2024.132853
[24] Craig DB, Dombkowski AA. Disulfide by Design 2.0: A web-based tool for disulfide engineering in proteins. BMC Bioinformatics, 2013, 14, 346. DOI: 10.1186/1471-2105-14-346
[25] Ferrada E, Wiedmer T, Wang WA, Frommelt F, Steurer B, Klimek C, et al. Experimental and computational analysis of newly identified pathogenic mutations in the creatine transporter SLC6A8. Journal of Mollecular Biolology, 2024, 436(2), 168383. DOI: 10.1016/j.jmb.2023.168383
[26] Buchan DWA, Jones DT. The PSIPRED protein analysis workbench: 20 years on. Nucleic Acids Research, 2019, 47(W1), W402-W407. DOI: 10.1093/nar/gkz297
[27] Varadi M, Anyango S, Deshpande M, Nair S, Natassia C, Yordanova G, et al. AlphaFold protein structure database: Massively expanding the structural coverage of protein-sequence space with high-accuracy models. Nucleic Acids Research, 2022, 50(D1), D439-D444. DOI: 10.1093/nar/gkab1061
[28] Ko J, Park H, Heo L, Seok C. GalaxyWEB server for protein structure prediction and refinement. Nucleic Acids Research, 2012, 40(W1), W294-W297. DOI: 10.1093/nar/gks493
[29] Wiederstein M, Sippl MJ. ProSA-web: Interactive web service for the recognition of errors in three-dimensional structures of proteins. Nucleic Acids Research, 2007, 35(suppl_2), W407-W410. DOI: 10.1093/nar/gkm290
[30] Butt SS, Badshah Y, Shabbir M, Rafiq M. Molecular docking using chimera and autodock vina software for nonbioinformaticians. JMIR Bioinformatics and Biotechnology, 2020, 1(1), e14232. DOI: 10.2196/14232
[31] Kozakov D, Hall DR, Xia B, Porter KA, Padhorny D, Yueh C, et al. The ClusPro web server for protein-protein docking. Nature Protocols, 2017, 12(2), 255-278. DOI: 10.1038/nprot.2016.169
[32] Yan Y, Zhang D, Zhou P, Li B, Huang SY. HDOCK: A web server for protein-protein and protein-DNA/RNA docking based on a hybrid strategy. Nucleic Acids Research, 2017, 45(W1), W365-W373. DOI: 10.1093/nar/gkx407
[33] López-Blanco JR, Aliaga JI, Quintana-Ortí ES, Chacón P. iMODS: Internal coordinates normal mode analysis server. Nucleic Acids Research, 2014, 42(W1), W271-W276. DOI: 10.1093/nar/gku339
[34] Hasan M, Ahmed S, Imranuzzaman M, Bari R, Roy S, Hasan MM, et al. Designing and development of efficient multi-epitope-based peptide vaccine candidate against emerging avian rotavirus strains: A vaccinomic approach. Journal of Genetic Engineering and Biotechnology, 2024, 22(3), 100398. DOI: 10.1016/j.jgeb.2024.100398
[35] Ali A, Alamri A, Mishra VK, Utegenova A, Askarova G, Baiduissenova A, et al. TZ1391: A computationally designed circular mRNA multi-epitope vaccine candidate against Mycobacterium tuberculosis via TLR3 immunomodulation. BMC Immunology, 2026, 27(1), 23. DOI: 10.1186/s12865-025-00795-4
[36] Ali A. Development of mRNA cancer vaccines: Delivery strategies and immunogenicity optimization. Current Medical Science, 2025, 45, 1275-1287. DOI: 10.1007/s11596-025-00127-y
[37] Computational prediction of HCV RNA polymerase inhibitors from Alkaloid library. Letters in Applied NanoBioScience, 2021. DOI: 10.33263/lianbs113.36613671
[38] Matarrese MAG, Loppini A, Nicoletti M, Filippi S, Chiodo L. Assessment of tools for RNA secondary structure prediction and extraction: A final-user perspective. Journal of Biomoleclar Structure & Dynamics, 2023, 41(14), 6917-6936. DOI: 10.1080/07391102.2022.2116110
[39] Bravi B. Development and use of machine learning algorithms in vaccine target selection. NPJ Vaccines, 2024, 9(1), 15. DOI: 10.1038/s41541-023-00795-8
[40] Diez M, Medina-Muñoz SG, Castellano LA, da Silva Pescador G, Wu Q, Bazzini AA. iCodon customizes gene expression based on the codon composition. Scientific Reports, 2022, 12(1), 12126. DOI: 10.1038/s41598-022-15526-7
[41] Castiglione F, Bernaschi M. C-immsim: playing with the immune response. Proceedings of the sixteenth international symposium on mathematical theory of networks and systems (MTNS2004). Katholieke Universiteit Leuven Belgium, 2004.
[42] Moin AT, Ullah MA, Patil RB, Faruqui NA, Araf Y, Das S, et al. A computational approach to design a polyvalent vaccine against human respiratory syncytial virus. Scientific Reports, 2023, 13(1), 9702. DOI: 10.1038/s41598-023-35309-y
[43] Bhattacharjee A, Hosen MR, Lamisa AB, Ahammad I, Chowdhury ZM, Jamal TB, et al. An integrated comparative genomics, subtractive proteomics and immunoinformatics framework for the rational design of a Pan-Salmonella multi-epitope vaccine. PLoS One, 2024, 19(7), e0292413. DOI: 10.1371/journal.pone.0292413

[44] Elalouf A, Maoz H, Rosenfeld AY. Bioinformatics-driven mRNA-based vaccine design for controlling tinea cruris induced by trichophyton rubrum. Pharmaceutics, 2024, 16(8), 983. DOI: 10.3390/pharmaceutics16080983
[45] Hu D, Irving AT. Massively-multiplexed epitope mapping techniques for viral antigen discovery. Frontiers in Immunology, 2023, 14, 1192385. DOI: 10.3389/fimmu.2023.1192385
[46] Wang BY, Hu SJ, Fu XN, Li LQ. $CD4^+$ cytotoxic T lymphocytes in cancer immunity and immunotherapy. Advanced Biology, 2023, 7(4), 2200169. DOI: 10.1002/adbi.202200169
[47] Rivera-Orellana S, Ramirez-Iglesias JR, Acosta-Espana JD, Espinosa-Espinosa J, Navarro JC, Herrera-Yela A, et al. Mpox vaccine design through immunoinformatics and computational epitope prediction. bioRxiv, 2024, 2011-2024. DOI: 10.1101/2024.11.05.622158
[48] Wang J, Jiang F, Cheng P, Ye ZY, Li L, Yang L, et al. Construction of novel multi-epitope-based diagnostic biomarker HP16118P and its application in the differential diagnosis of Mycobacterium tuberculosis latent infection. Molecular Biomedicine, 2024, 5(1), 15. DOI: 10.1186/s43556-024-00177-z
[49] Silva MF, Pereira G, Mateus L, da Costa LL, Silva E. Design of a multi-epitope-based vaccine candidate against Bovine Genital Campylobacteriosis using a reverse vaccinology approach. BMC Veterinary Research, 2024, 20(1), 144. DOI: 10.1186/s12917-024-04006-x
[50] Jalal K, Khan K, Uddin R. Immunoinformatic-guided designing of multi-epitope vaccine construct against Brucella Suis 1300. Immunologic Research, 2023, 71(2), 247-266. DOI: 10.1007/s12026-022-09346-0
[51] Shahab M, Aiman S, Alshammari A, Alasmari AF, Alharbi M, Khan A, et al. Immunoinformatics-based potential multi-peptide vaccine designing against Jamestown Canyon Virus (JCV) capable of eliciting cellular and humoral immune responses. International Journal of Biological Macromolecules, 2023, 253(Pt 2), 126678. DOI: 10.1016/j.ijbiomac.2023.126678
[52] Gupta K. *In silico* structural and functional characterization of hypothetical proteins from Monkeypox virus. Journal of Genetic Engineering and Biotechnology, 2023, 21(1), 46. DOI: 10.1186/s43141-023-00505-w
[53] McGuffin LJ, Bryson K, Jones DT. The PSIPRED protein structure prediction server. Bioinformatics, 2000, 16(4), 404-405. DOI: 10.1093/bioinformatics/16.4.404
[54] Alharthi F, Althagafi HA, Jafri I, Oyouni AAA, Althaqafi MM, Al-Hazmi NE, et al. Enhanced biochemical properties of soybean root nodule asparaginase through plant molecular farming compared to bacterial enzyme for cancer treatment. Rhizosphere, 2024, 32, 100970. DOI: 10.1016/j.rhisph.2024.100970
[55] Varadi M, Bertoni D, Magana P, Paramval U, Pidruchna I, Radhakrishnan M, et al. AlphaFold protein structure database in 2024: Providing structure coverage for over 214 million protein sequences. Nucleic Acids Research, 2024, 52(D1), D368-D375. DOI: 10.1093/nar/gkad1011
[56] Riel AMS, Rungelrath V, Elwaie TA, Rasheed OK, Hicks L, Ettenger G, et al. Systematic evaluation of regiochemistry and lipidation of aryl trehalose mincle agonists. International Journal of Molecular Sciences, 2024, 25(18), 10031. DOI: 10.3390/ijms251810031
[57] De Vries SJ, Van Dijk M, Bonvin AMJJ. The HADDOCK web server for data-driven biomolecular docking. Nature Protocols, 2010, 5(5), 883-897. DOI: 10.1038/nprot.2010.32
[58] Mandal M, Mandal S. MM-GBSA and QM/MM simulation-based *in silico* approaches for the inhibition of Acinetobacter baumannii class D OXA-24 β-lactamase using antimicrobial peptides melittin and RP-1. Chemical Physics Impact, 2024, 8, 100401. DOI: 10.1016/j.chphi.2023.100401
[59] Ali SL, Ali A, Alamri A, Baiduissenova A, Dusmagambetov M, Abduldayeva A. Genomic annotation for vaccine target identification and immunoinformatics-guided multi-epitope-based vaccine design against Songling virus through screening its whole genome encoded proteins. Frontiers in Immunology, 2023, 14. DOI: 10.3389/fimmu.2023.1284366
[60] Varenyk Y, Spicher T, Hofacker IL, Lorenz R. Modified RNAs and predictions with the viennaRNA package. Bioinformatics, 2023, 39(11), btad696. DOI: 10.1093/bioinformatics/btad696
[61] Hong W, Chen C, Zhu Z, Tang K. An elite archive-sssisted multi-objective evolutionary algorithm for mRNA design. IEEE Congress on Evolutionary Computation, 2024, 1-8. DOI: 10.1109/CEC60901.2024.10611972
[62] Ranjan VV, Leighton GO, Yan C, Arango M, Lustig J, Corona RI, et al. DNA binding and transposition activity of the Sleeping Beauty transposase: role of structural stability of the primary DNA-binding domain. Nucleic Acids Research, 2024, gkae1188. DOI: 10.1093/nar/gkae1188
[63] Liu YY, Li YC, Hu QX. Advances in saRNA vaccine research against emerging/re-emerging viruses. Vaccines, 2023, 11(7), 1142. DOI: 10.3390/vaccines11071142
[64] Guan YJ, Li M, Qiu ZD, Xu JH, Zhang YC, Hu N, et al. Comprehensive analysis of DOK family genes expression, immune characteristics, and drug sensitivity in human tumors. Journal of Advanced Research, 2022, 36, 73-87. DOI: 10.1016/j.jare.2021.06.008
[65] Khan MS, Shamsi A, Zuberi A, Shahwan M. *In silico* repurposing of FDA-approved drugs against MEK1: Structural and dynamic insights into lung cancer therapeutics. Frontiers in Pharmacology, 2025, 16, 1619639. DOI: 10.3389/fphar.2025.1619639
[66] Ali A, Ali SL, Alamri A, Khatrawi EM, Baiduissenova A, Suleimenova F, et al. Multi-epitope-based vaccine models prioritization against Astrovirus MLB1 using immunoinformatics and reverse vaccinology approaches. Journal of Genetic Engineering and Biotechnology, 2025, 23(1), 100451. DOI: 10.1016/j.jgeb.2024.100451
[67] Minnaert AK, Vanluchene H, Verbeke R, Lentacker I, De Smedt SC, Raemdonck K, et al. Strategies for controlling the innate immune activity of conventional and self-amplifying mRNA therapeutics: Getting the message across. Advanced Drug Delivery Reviews, 2021, 176, 113900. DOI: 10.1016/j.addr.2021.113900
[68] Jung HN, Lee SY, Lee S, Youn H, Im HJ. Lipid nanoparticles for delivery of RNA therapeutics: Current status and the role of *in vivo* imaging. Theranostics, 2022, 12(17), 7509-7531. DOI: 10.7150/thno.77259